Comparisons of measured nitrous acid (HONO) concentrations in a pollution period at urban and suburban Beijing, in autumn of 2014

Shengrui Tong[1*], Siqi Hou[1], Ying Zhang[1], Biwu Chu[2], Yongchun Liu[2], Hong He[2], Pusheng Zhao[3] & Maofa Ge[1*]

[1]*State Key Laboratory for Structural Chemistry of Unstable and Stable Species; Beijing National Laboratory for Molecular Sciences; Institute of Chemistry, Chinese Academy of Sciences, Beijing 100190, China*
[2]*Research Center for Eco-Environmental Sciences, Chinese Academy of Sciences, Beijing 100085, China*
[3]*Institute of Urban Meteorology, China Meteorological Administration, Beijing 100089, China*

To study the HONO formation mechanisms during a pollution period, a continuous measurement was performed in both urban and suburban aeras of Beijing. During this period, the $PM_{2.5}$ concentrations increased to 201 and 137 μg/m^3 in urban and suburban areas, respectively. The concentrations of HONO, CO, SO_2, O_3, NO, NO_2, NO_x were 1.45 ppbv, 0.61 ppmv, 8.7 ppbv, 4.3 ppbv, 44.4 ppbv, 37.4 ppbv, 79.4 ppbv and 0.72 ppbv, 1.00 ppmv, 1.2 ppbv, 7.9 ppbv, 3.7 ppbv, 8.2 ppbv, 11.9 ppbv, in urban and suburban areas, respectively. To compare possible pathways of HONO formation in both sites, the contributions of direct emissions, heterogeneous formations, and homogeneous productions were studied. $HONO/NO_2$ ratios in the two sites indicated that heterogeneous reactions of NO_2 were more efficient in suburban areas. And in both urban and suburban areas, the increase of $PM_{2.5}$ concentrations and *RH* would promote the conversion efficiency in *RH* that ranged from 0% to 85%. However, when *RH* was above 85%, the HONO formation slowed down. Moreover, the study of direct emissions and homogeneous reactions showed that they contributed to a majority of HONO increase in urban areas than the 20% contributions in suburban areas. It implied that the high NO_x concentrations and NO concentrations in urban areas or in pollution periods would make direct emissions and homogeneous reactions become dominant in HONO formations.

nitrous acid, pollution, urban, suburban, comparison

1   Introduction

Nitrous acid (HONO) is one of the important species in photochemical cycles, which could provide hydroxyl radical (OH) [1,2] with contributions up to 30%–50% [3,4]. OH radical, one of the most improtant oxidant in the atmosphere, can react with organic matters, enhance the capacity of atmospheric oxidation, lead to the formation of secondary pollutants, and accelerate the formation of air pollutions [2].

Therefore, the study on the HONO formation mechanism will be helpful to understand the complex process during pollution. The genarally accepted sources of HONO were direct emissions, homogeneous reaction of NO and OH, and heterogeneous reaction of NO_2 [4]. HONO could be emitted directly by combustion processes, with quantities about 0.3%–0.8% of NO_x (NO+NO_2) obtained by tunnal studies [5,6]. The direct emission sources were seen to be unimportant except in high NO_x regions and traffic hours [7]. The homogeneous reaction of NO and OH was also one of the HONO formation sources. It was normally seen as less important due to its low prodution rate [1], but the high

concentrations of OH and NO in pollution strengthened the importance of this reaction source. Laboratory studies indicated that NO_2 heterogeneous reactions on humid surfaces can be used to explain parts of the HONO formation [8–11]. The reaction efficiency depended on the surface absorbed water, the surface compositions, and the surface types [11]. However, the mechanism was still in argument due to the differences between laboratory and field measurements [11].

The field observations of HONO were performed in various locations including remote areas, rural areas, suburban and urban areas [3,7,11–25]. Results showed that HONO concentrations were lower in remote places and clean areas. Due to heavy pollution, the HONO concentrations were much higher in mega cities of China. Moreover, the differences of HONO concentrations also lied in urban and suburban areas. For example, it was 1.45 ppbv [18] in urban and 0.89 ppbv [15] in suburban areas of Beijing, 3.50 ppbv [16] in urban and 0.95 ppbv [7] in rural areas of Guangzhou, 1.50 ppbv [14,23] in urban and 1.30 ppbv [20] in non-urban areas in Shanghai. As the indicator of heterogeneous reaction extent, $HONO/NO_2$ ratios were also different in various places. Normally it was in the range of 0.01 to 0.13 [14,15,17–20], and could reach up to 0.175 [7] and 0.35 [16] at Guangzhou, and 0.42 [25] in Kathmandu with high relative humidity.

The differences in HONO concentrations may be caused due to various reasons in recent China [26–28]. And the measurements in different areas could be helpful to understand the formation mechanism of HONO and the important impacts on HONO in the pollution process. Therefore, in present work, a continuous measurement was performed in the urban and suburban areas of Beijing from October 28 to November 2, with high pollution in both areas. From this measurement, the concentrations of HONO and SO_2, O_3, CO, NO_x in urban and suburban areas were obtained. Diurnal variations of gaseous species as well as the changing meteorological conditions were analyzed. Moreover, HONO formation sources from direct emissions, homogeneous reactions and heterogeneous reactions in both sites were discussed and different formation mechanisms were obtained.

2   Materials and methods

2.1   Measurement sites

In this work, as a comparison was performed in urban and suburban areas of Beijing, two sites were chosen for the study.

(1) For the urban area. The HONO measurement was performed at the platform in the third floor in No.2 building of Institute of Chemistry, Chinese Academy of Sciences (ICCAS, 116°19′21.58″E, 39°59′22.68″N). The ICCAS site

is located at the North Fourth Ring Road of Haidian District, which could be seen as a typical urban area with condensed population and heavy traffic. In addition, the gas phase pollutants of CO, SO_2, O_3, NO, NO_2 and NO_x were measured by commercial SO_2 analyzer (43i, Thermo, USA), O_3 analyzer (49i, Thermo, USA), NO_x analyzer (42i, Thermo, USA) and CO analyzer (48i, Thermo, USA) with detection limits of 1 ppbv, 1 ppbv, 1 ppbv and 0.05 ppmv, respectively. The analyzers were installed at Baolian, 5.5 kilometers southwest from the ICCAS site with similar conditions and little spatial differentiations of NO_2 and NO_x concentrations [29]. Meteorological parameters, including wind speed, wind directions, temperature, pressure, relative humidity and $PM_{2.5}$ concentrations were obtained from http://www.weather.com.cn/weather/101010100.shtml   in Baolian station.

(2) For the suburban area. The HONO analyzer and other gas analyzers were settled at the 4th floor of the first classroom building in the Lake yanqi campus of University of Chinese Academy of Sciences (UCAS, 40.4°N, 116.6°E). The UCAS was 50 km northeast of the city center, and in the west side of the Jingjia highway and was in the northeast of Lake Yanqi within 1 km, which could be an example of suburban area. The gaseous species of CO, SO_2, O_3, NO, NO_2 and NO_x were measured by analyzers as used in the urban site. And meterological parameters were also obtained from http://www.weather.com.cn/weather/101010 100.shtml in Huairou station.

2.2   Measurement instruments of HONO

During the experiment, the HONO concentrations were measured by a home-made HONO analyzer in each site. The mechanism of the analyzer was based on long path-length absorbance spectroscopy [30,31]. HONO was absorbed by a solution containing 0.06 mol/L sulfanilamide in 1 mol/L HCl [32], and then formed an azo dye by reacting with a dye solution (0.8 mmol/L *N*-(1-naphthyl) ethylene-diaminedihydrochloride) [31]. The azo dye was pumped into 250 cm Teflon absorption cells (Liquid Core Waveguide, LCW) [30] and detected by a mini-spectrometer with a diode array detector (Ocean Optics, SD2000) [32]. The gas collecting device was designed to be of two channels, which could get a real HONO concentration by subtracting the interferences [30]. The sampled gas flow rate was 1 L/min with the solutions liquid flow rate of 0.5 mL/min. The detection limit of the HONO analyzer was 9 pptv with a response time (the time of the instrument rising to 90% of the full signal) of 5 min. Moreover, an inter-comparison of the two home-made HONO analyzers used in each site was performed. And the differences of measured concentrations lied within 0.008, which indicated the concentrations measured by the two HONO analyzers in the two sites were reliable and comparable.

3 Results and discussion

3.1 Time series of meteorological parameters and measured gases species

The measured meteorological parameters, i.e., air temperature (T), relative humidity (RH), wind speed (WS) and direction (WD) as well as the PM$_{2.5}$ concentrations were illustrated in Figure 1. According to the National Ambient Air Quality Standard (ambient air quality standards which is to be implemented in 2016: GB3095-2012), two successive days with the daily mass concentration of PM$_{2.5}$ exceeding 75 µg/m^3 were defined as an air pollution episode. Therefore, a heavy pollution occurred from the midnight of Oct. 29 to the early morning in Nov. 1 at the urban area of Beijing, with average PM$_{2.5}$ mass concentration of 150 µg/m^3. Whereas, the pollution period in suburban areas was from 9:00 LTS in Oct. 29 to the midnight of Oct. 31, with the average PM$_{2.5}$ concentration of 103 µg/m^3.

Moreover, during the pollution period, the variations of temperatures, wind speeds and the relative humidities were similar between the two sites. The meterological parameters are listed in Table 1. In urban and surburban sites, the temperature was from 4.5 to 16.4 °C and from 1.7 to 16.7 °C, the relative humidity range was from 47% to 100% and from 34% to 100%, the wind speed was with a mean value of 0.56 and 0.96 m/s, respectively. However, the PM$_{2.5}$ concentrations in the two sites were different: (1) the max hourly averaged PM$_{2.5}$ concentrations was 201 and 137 µg/m^3, in urban and suburban areas, respectively; (2) the growth rate of PM$_{2.5}$ concentations were much higher in

urban areas; (3) 4 significant peaks were observed in urban areas, while only 3 peaks in the suburban areas. After the pollution period, the meterological conditions changed in both sites from Nov. 1 with stronger wind speeds and lower relative humidities.

Figure 2 shows the time series of the concentrations measured in each site during the observation period. The average concentrations of the measured gaseous pollutants in both sites are listed in Table 2. HONO was from 0.54 to 2.77 ppbv with the average of 1.45 ppbv in urban area, and from 0.18 to 1.23 ppbv with the average of 0.74 ppbv in suburban area. In the studies of Spataro *et al*. [18], HONO concentration was 1.06 ppbv on average, with mean NO$_2$ concentration of 38.8 ppbv in urban Beijing. Hendrick *et al*. [15] showed a HONO concentration of 2 ppbv in urban area of Beijing with 1.25 ppbv at the same time in Xianghe. Moreover, during the period from Oct. 28 to Oct. 31, the max HONO concentrations had a decreasing trend in urban areas, while increasing in the surburban areas. The average concentrations of NO, NO$_2$, NO$_x$ and SO$_2$ in urban areas were much higher than that in suburban areas except the concentrations of CO and O$_3$. It was interesting that the concentrations of CO, NO and NO$_x$ in urban areas showed similar variations with peaks at night and minimum in the afternoon, while these correlations were not significant for the suburban areas. During the pollution period, the hourly averaged concentrations of NO, NO$_2$, NO$_x$, and HONO in urban areas were equally 12.7, 4.5, 6.6, and 2.0 times higher, and SO$_2$, CO, O$_3$ were 7.9, 1.7 and 1.8 times lower than in suburban areas.

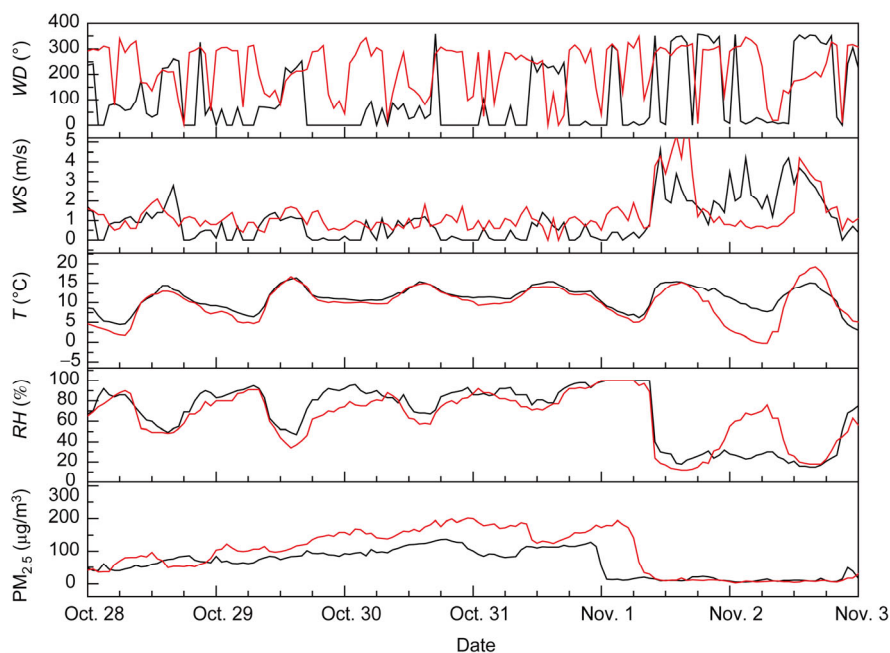Furthermore, these species had clear diurnal variations in

Figure 1 Time series of hourly-averaged air temperature (T), relative humidity (RH), wind speed (WS) and direction (WD) and PM$_{2.5}$ concentrations during Oct. 28 to Nov. 2, 2014. Red lines represent the results from urban station, while the black ones represent the results from suburban station.

Table 1 Summary of the meterological parameters and $PM_{2.5}$ concentrations in urban and suburban sites

	WD	WS (m/s)	T (°C)	RH (%)	$PM_{2.5}$ ($\mu g/m^3$)
Urban [a]	North	0–2.8	4.5–16.4	47–100	36–201
Suburban [a]	Northwest	0–2.1	1.7–16.7	34–100	40–137

a) Data obtained from http://www.weather.com.cn/weather/101010 100.shtml.
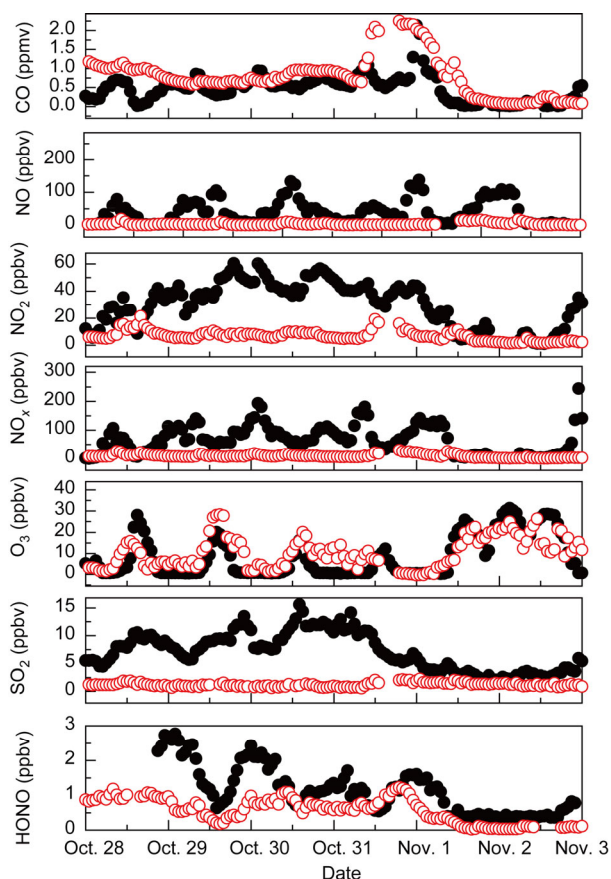
Figure 2 Temporal variations of CO, SO_2, O_3, NO, NO_2, NO_x, and HONO in 1-h average during Oct. 28 to Nov. 2, 2014. The solid points represent the results from urban areas, while the hollow ones represent the results from suburban areas.

Table 2 Daytime and nighttime average concentrations of the measured chemical species in urban and suburban areas

Species	Daytime [a] (ppbv) suburban/urban	Nighttime [b] (ppbv) suburban/urban	Total (ppbv) suburban/urban
HONO	0.73/0.93	0.72/1.75	0.74/1.45
SO_2	1.3/9.6	1.1/8.1	1.2/8.7
CO	1.00/0.48	1.04/0.68	1.0 /0.61
O_3	11.5/10.3	4.9/1.3	7.9/4.3
NO	1.9/19.1	4.4/56.9	3.8/44.4
NO_2	11.3/35.3	6.7/37.6	8.4/37.4
NO_x	13.2/53.4	11.0/8.6	11.9/79.4

a) Daytime: 09:00–17:00 LST; b) nighttime: 19:00–7:00 LST.

both urban and suburban areas (Figure 3). The variations of HONO concentrations have differences between urban and suburban areas. For the urban area, HONO kept decreasing by photolysis after 7:00 AM and reached minimum at around 15:00 PM. Then it grew slowly during the rest of the day, and maintained high concentrations through all night until next morning. However, in the suburban area, HONO concentration changed more gently in both daytime and nighttime except two peaks around 9:00 AM and 19:00 PM, respectively. It may be associated with the local traffic according to both NO_2 and NO_x peaks at the same time. The CO had clear diurnal variations with higher values at night and lower values at daytime as similar to the variations of NO_x and NO in urban areas. All of them showed significant peaks in the morning, and decreased during the daytime until 15:00 LST, then increased during the night with maximums at midnight. In the suburban area, unlike the slight changing of CO, the NO_x and NO showed typical peaks at around 9:30 LST in the morning and 1:00 LST at midnight. The SO_2 decreased from the midnight and increased at 6:00 until 14:00 LST in urban area, then had little changes the rest of the day. While in the suburban area, the increasing time of SO_2 was delayed to 8:00, and decreased from 16:00. In the urban area, the NO_2 concentrations were higher at
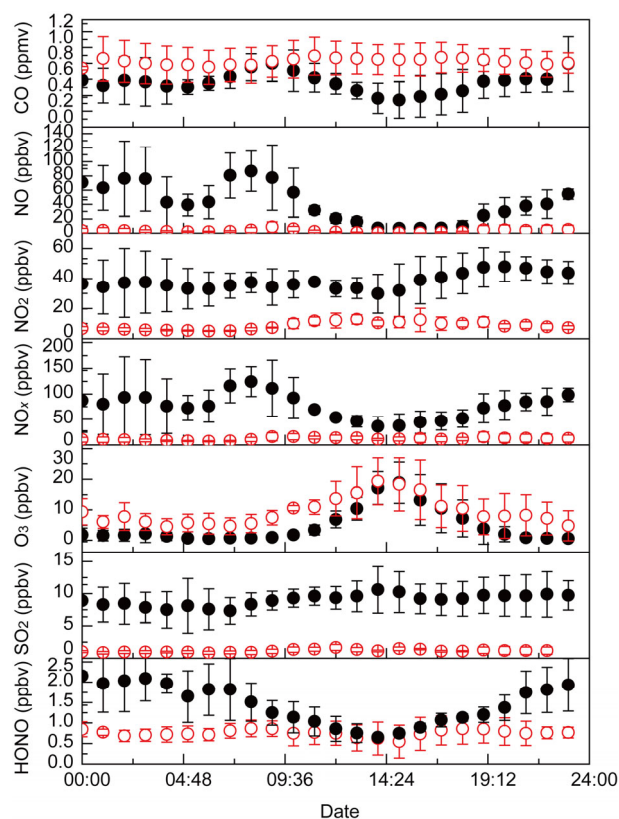
Figure 3 Average diurnal patterns of CO, NO, NO_2, NO_x, O_3, SO_2 and HONO during the measurement period. The data was calculated by averaging the concentrations of Oct. 28–Oct. 31, 2014. The error bars represent the standard deviation within the measurement period. The solid points represent the results from urban site, while the hollow ones represent the results from suburban site.

night and lower at day, while the variations in suburban area were opposite to that. NO_2 increased at 8:00 in the morning and kept high values until 19:00 LST. The higher NO_2 was caused by the oxidation of the emitted NO around 10:00 LST. Although the max values of O_3 in the two sites were similar, the increasing time was delayed from 8:00 to 11:00 LST in urban areas.

The similar variations of gases pollutants may indicate similar sources of them [3,18]. Therefore, the sources of CO, NO, and NO_x were similar in urban areas, while they were more complicated in suburbans. Normally, CO and NO_x were mainly from combustion processes including the burning of fossil fuel and biomass, as well as vehicle emissions [26–28]. The sources of SO_2 would mainly come from the burning of fossil fuel and biomass, which often happened in the suburban [26]. Therefore, the good correlations of CO and NO_x in urban areas may be caused by the life sources and the mobile sources [28], like vehicle emissions; and the weak correlations of CO, NO_x and SO_2 in suburban areas may be caused by a combination of fossil fuel burning, biomass burning, vehicle emissions and other combustion processes.

3.2   The impact factors on HONO formation

3.2.1   The direct emissions

For the evaluation of direct HONO formation sources, relationships between HONO with CO, NO_x and SO_2 were studied (Figures 4–6). The correlations of HONO with CO, NO_x, and SO_2 were 0.597 and 0.665, 0.679 and 0.439, 0.380 and 0.022 for the urban area and the suburban area, respectively. Therefore, the HONO sources in urban areas were partly connected with the sources of CO, NO_x and SO_2 [3,18]. While in the suburban areas, the HONO sources were connected with the sources of CO and NO_x. Although both of the measurement sites were closed to a traffic source, the traffic flows and types were different. The traffic close to the urban site was much higher with mainly passenger cars, however, the traffic at the suburban site was more complicated, where the train station, small factories and farmland were not far away. Moreover, the existence of Lake Yanqi may also have effects on the surrounding conditions.

The HONO/NO_x ratio was used to evaluate the amounts by direct emissions in the atmosphere [3]. The HONO/NO_x
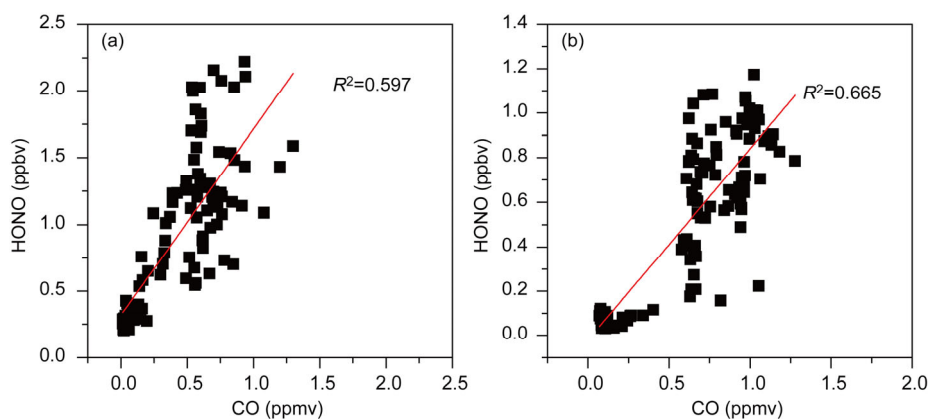

Figure 4   The correlations between HONO and CO in urban site (a) and suburban site (b), by using the data from Oct. 28 to Oct. 31, 2014.
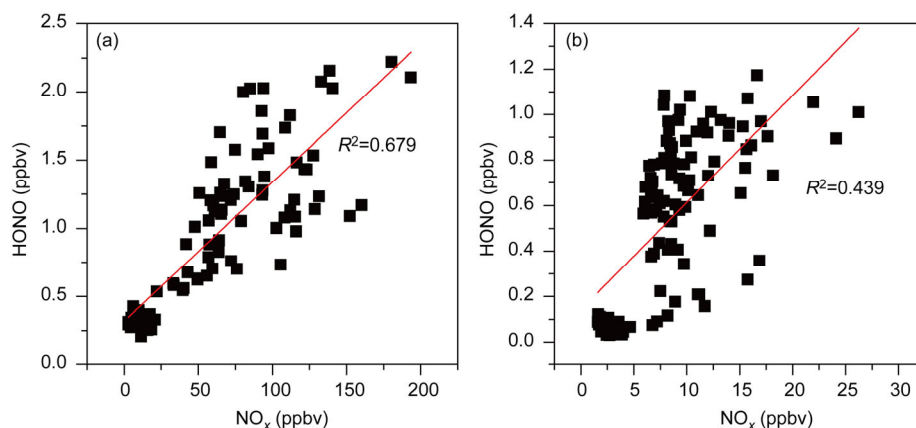

Figure 5   The correlations between HONO and NO_x in urban site (a) and suburban site (b), by using the data from Oct. 28 to Oct. 31, 2014.
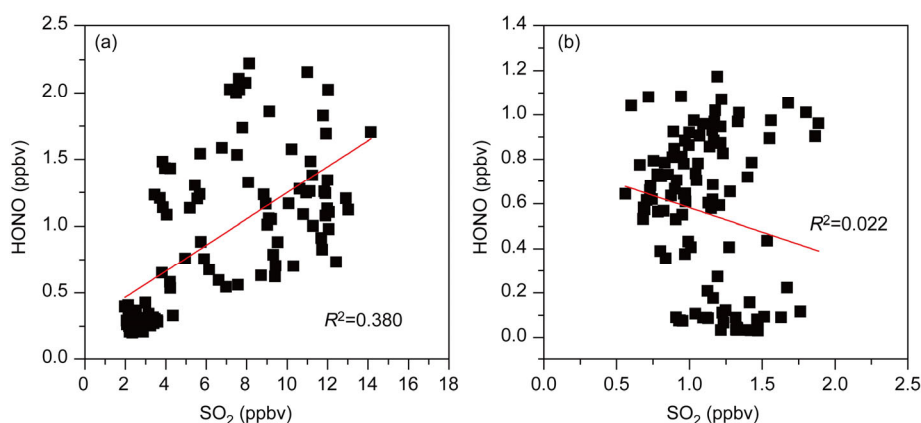
Figure 6   The correlations between HONO and SO_2 in urban site (a) and suburban site (b), by using the data from Oct. 28 to Oct. 31, 2014.

ratio of 0.0065 as the direct emission factor supported by Kurtenbach *et al*. [5] was widely accepted in most recent studies [7,18–24]. In this work, the average HONO/NO_x ratios during the pollution period obtained in urban and suburban areas were 0.017 and 0.070, respectively. The HONO/NO_x ratios showed two peaks in consistance with the morning and evening traffic hours in urban areas, which were caused by the emissions of vehicle exhausts. However, all these measured HONO/NO_x ratios were much higher than the direct emission factor of 0.0065. It is implied that, the HONO in the ambient atmosphere not only comes from direct emissions, but also comes from secondly formation and other pathways. Therefore, 0.0065 was used to calculate the direct emissions concentrations of HONO ($HONO_{emission}$) by the formula: $[HONO_{emission}]=[NO_x]\times 0.0065$ [16,18]. Where, $[HONO_{emission}]$ and $[NO_x]$ represented HONO concentrations by direct emissions and the concentrations of NO_x, respectively. The calculated $HONO_{emissions}$ was with contributions of 39.6% and 8.5% on average, in urban and suburban areas, respectively. In previous studies, the contributions of $HONO_{emission}$ could be 49.7% with 266 ppbv NO_x in urban Beijing [18]. The comparison of $HONO_{emissions}$ in both sites in this measurement indicated that direct emissions are more important in urban areas.

3.2.2   The nocturnal heterogeneous reaction of NO_2

It was well-accepted that HONO could be formed on the wet surface by heterogeneous conversion of NO_2 [3,8–11, 33]. The conversion rate may be affected by the aerosol surfaces and the surface water [10–12,14,19,33]. Therefore, the influence of $PM_{2.5}$ and *RH* were important to explore the heterogeneous reaction mechanism. Lab studies had shown that the reaction was first order in NO_2 [10], and HONO/NO_2 ratio was usually used to evaluate the extent from the heterogeneous reaction of NO_2 [3,7,12,16,18]. Nighttime HONO/NO_2 ratios in urban cities of China were from 0.03 to 0.15 [7,12,14,20,23], higher ratios were obtained in Guangzhou with high relative humidity [7,16]. In this measurement, the variations of nocturnal HONO/NO_2 ratios

in both urban and suburban areas were plotted in Figure 7. To avoid the uncertainties caused by the photolysis reaction in daytime, all the daytime data (from 7:00 LST to 18:00 LST) were ignored [11,20]. During the nighttime, the average HONO/NO_2 ratio was 0.044 and 0.110, in urban and suburban areas, respectively. The higher ratios of HONO/NO_2 in suburbans indicated higher conversion efficiency of NO_2 heterogeneous reactions [11,33]. The heterogeneous formation of HONO could have occurred on various surfaces with different conversion rates, and the preferences to aerosol or ground surface were still in discussions [34]. However, compared to the urban surfaces of concrete, glass and foliage, the suburban surroundings provided much more surfaces for the heterogeneous reactions such as soils, lake, mineral dusts as well as numerous particles [34]. These factors may result in the high heterogeneous reaction efficiency in suburban areas. The heterogeneous reaction of NO_2 could be affected by NO_2 concentrations, relative humilities, the boundary layer heights, aerosol concentrations, the reactive surfaces and so on [25,33]. And then the effects of relative humidity and $PM_{2.5}$ concentrations were studied.

Stutz *et al*. [11] pointed out that the absorbed water had influences on heterogeneous formation of HONO with independence on surfaces types. In other studies [7,11,12,14, 15,18,23,25,33], HONO/NO_2 ratios were ~0.03 on dry surfaces, increasing to 0.10–0.13 on wet surfaces. However, HONO/NO_2 ratios on aqueous surfaces were uncertain [11,33]. In this measurement, it could be clearly identified in the suburban that (Figure 8), the HONO/NO_2 ratios increased from 0.02 to 0.15 with *RH* from 0 to 85%, and when the *RH* was up to 85%, HONO/NO_2 ratios decreased to 0.10. The same phenomenon could also be seen in urban areas when *RH* was higher than 90%. However, the tendency was uncertain in the low *RH* range due to the scattered points in the picture. It indicated that the absorbed water had complex effects on the NO_2 heterogeneous formation of HONO. As a competition of HONO sources and sinks [9], the surface absorbed water could affect both processes of NO_2 to HONO and HONO deposition. When the
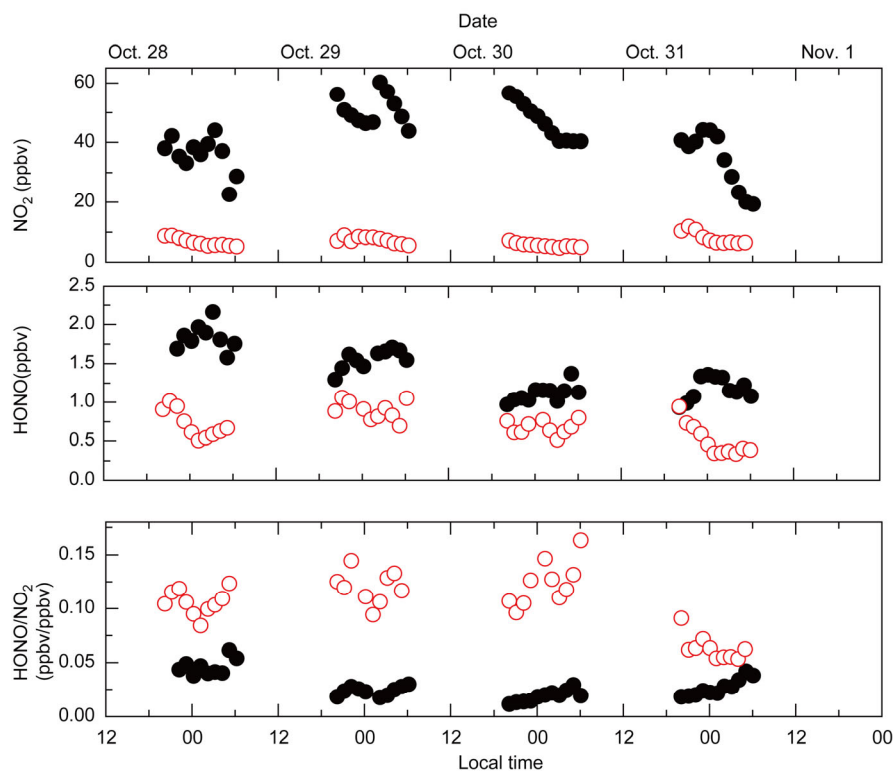
Figure 7   Time series of HONO/NO₂ ratios in the nighttime during the pollution period in urban area (black solid) and suburban (red hollow).
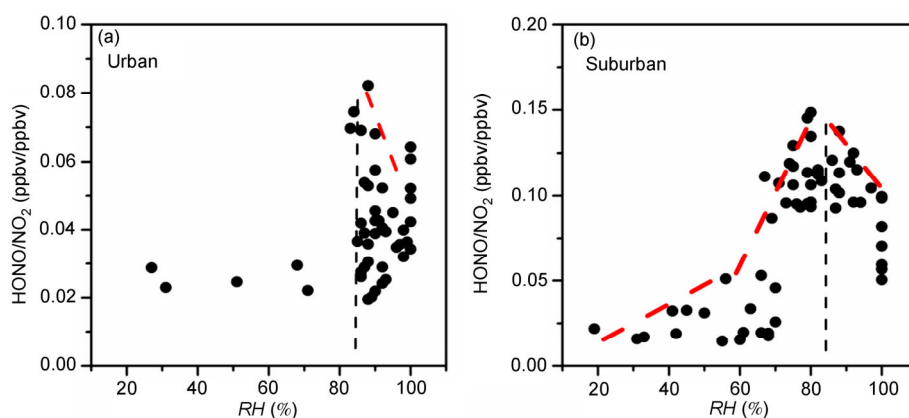

Figure 8   Correlations between HONO and *RH* in urban site (a) and suburban site (b).

RH was from 20% to 80%, the depositions of HONO would increase with *RH*. Moreover, the surface water coverage was increasing with *RH*. As the dependence on *RH* of the heterogeneous conversion was stronger than the HONO deposition [11], the conversion efficiency would increase as a result. However, when the surface became saturated (*RH*> 85%), the excess water could be a limiting reagent for NO₂ [33] and dissolution of HONO, which could result in a decrease in HONO/NO₂ ratios.

The particle mass concentration would also influence HONO heterogeneous formations [14,16]. To study this effect, correlations between HONO/NO₂ and PM₂.₅ were plotted (Figure 9). When the PM₂.₅ concentrations were lower than 100 μg/m³, the HONO/NO₂ ratios were increasing with the increase of PM₂.₅ concentrations both in urban and suburban areas. And the ratios declined after the PM₂.₅ concentrations were above 100 μg/m³. As seen in Figure 9, all the declining ratios were in high *RH* region (higher than 80%), in either urban or suburban area. So the decline of HONO/NO₂ ratios may be caused by the high content of absorbed water as it could be a limiting reagent for NO₂ conversions. Therefore, although the particle matters could promote the HONO formation, in high *RH* ranges, the highly absorbed water would lead to a HONO/NO₂ decrease [11].
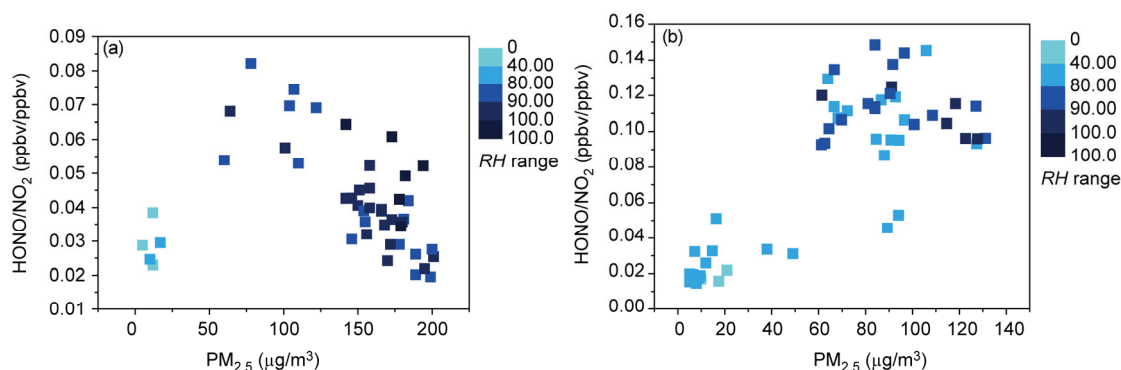
Figure 9   Correlations between HONO and PM$_{2.5}$ concentrations in urban site (a) and suburban site (b).

3.2.3   The nocturnal gas phase formation by NO and OH

The homogeneous reaction NO+OH→HONO (K_{NO+OH}= 9.8×10^{-12} cm^3/(molecules s)) and HONO+OH→NO$_2$+H$_2$O ($K_{HONO+OH}$=6.0×10^{-12} cm^3/(molecules s)) would dominate the homogeneous production of HONO in nighttime [4]. Therefore, the net HONO homogeneous production could be calculated by [3,4,7]:

$$P_{net}=K_{NO+OH}\times[NO]\times[OH]-K_{HONO+OH}\times[HONO]\times[OH].$$

where P_{net} represented the net homogeneous production rate of the reation NO+OH→HONO and HONO+OH→NO$_2$+ H$_2$O [3,4,7]; [] represented as the concentrations of gases. A nighttime OH concentrations of 1×10^6 molecules/cm^3 was assumed to represent the measured ones in both urban and suburban areas [18,35]. Since the reaction rates were similar, the P_{net} was mainly decided by the concentrations of NO and HONO. For the urban area, the P_{net} values were in proportion to NO concentrations, due to the high nocturnal NO concentrations. The average P_{net} in urban area was

much higher than in suburban area, which was 2.18 ppbv/h with the NO concentrations of 59.0 ppbv and 0.137 ppbv/h with NO concentrations of 4.6 ppbv, in urban and suburban areas, respectively. Such a high P_{net} value on urban areas would make the effect of homogeneous productions amazing. As shown in Figure 10, for the first night from 20:00 to 24:00, the mean P_{net} values in urban area increased from 1.31 to 2.58 ppbv/h with HONO increasing from 1.37 to 2.01 ppbv. Therefore, by integrating P_{net} in this 4 h [7], the homogeneous reactions could provide at least 0.27 ppbv accumulations of HONO, which was 42.2% of the measured increase of HONO (0.64 ppbv). In constrast to suburban areas, the low NO concentrations could only provide P_{net} from 0.126 to 0.213 ppbv/h with an integrating area of 0.020 ppbv, which was 10.6% of HONO increasing (0.187 ppbv). It indicated that, when the concentrations of NO were extremely high, the net productions by homogeneous reactions could be dominant for the nighttime increase of HONO and its contribution would even exceed the formation
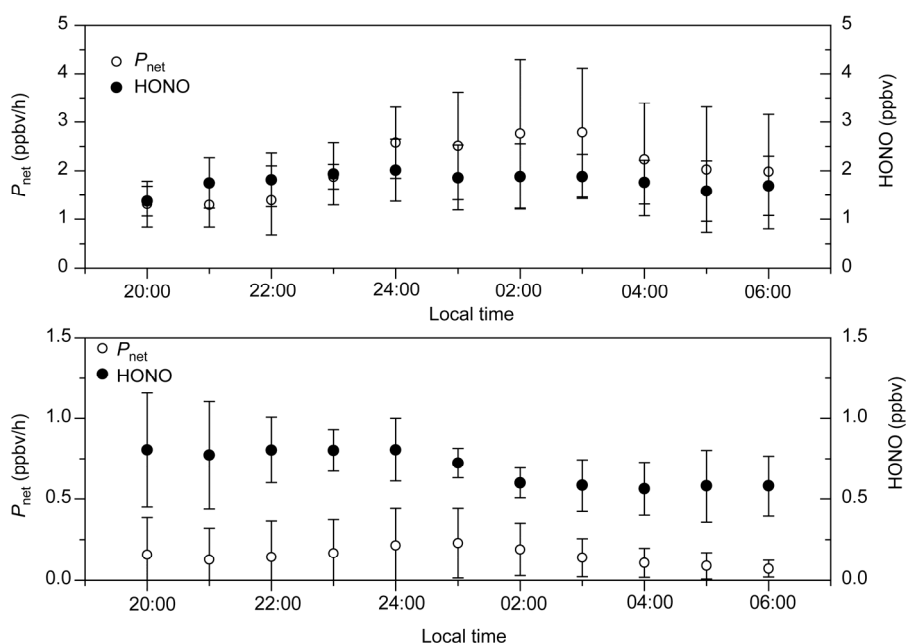

Figure 10   Average diurnal patterns of P_{net} and HONO in the nighttime during the measurement period.

by heterogeneous reactions [18].

To sum it up, the nocturnal HONO formation mechanisms in urban and suburban areas were different (Table 3). For the urban area, with the average contributions of 39.6% and 42.2%, the direct emissions and the net homogeneous production would provide 81.8% of HONO formation. While in the suburban area, the on average contributions of direct emissions and the net homogeneous production was 8.5% and 10.6%, respectively. Moreover, the mean HONO/NO_2 ratio in suburban area (0.103) was 2.7 times higher than 0.038 in urban areas, which was in agreement with the remaining contributions of HONO formations. Therefore, for the urban and suburban areas, the differences in NO_x concentrations, NO concentrations, relative humidity and $PM_{2.5}$ concentrations would lead to rather different HONO formations. The high NO_x concentrations would result in a high direct emissions of HONO, and the high NO concentrations would make the homogeneous reaction productions become significant. For the heterogeneous formations, particle concentrations and absorbed water on reactive surfaces would promote the HONO formation efficiency. In addition, higher *RH* values would make HONO dissolved in water and result in a decline of HONO/NO_2 ratios.

4   Conclusions

A comparison study on HONO formation was performed in urban and suburban areas during a pollution period based on a continuous measurement from Oct. 28 to Nov. 3, 2014 in Beijing. During the measurement, both the sites in urban and suburban areas suffered a pollution process with mean $PM_{2.5}$ concentrations of 130 and 85, respectively. The hourly-averaged concentrations of HONO, CO, SO_2, O_3, NO, NO_2, and NO_x in the pollution period were (1.45 ppbv, 0.61 ppmv, 8.7 ppbv, 4.3 ppbv, 44.4 ppbv, 37.4 ppbv, and 79.4 ppbv) much higher than concentrations in suburban (0.72 ppbv, 1.00 ppmv, 1.2 ppbv, 7.9 ppbv, 3.7 ppbv, 8.2 ppbv, and 11.9 ppbv). Correlations of HONO with CO, NO_x, and SO_2 showed similar sources between HONO and CO, NO_x in both areas, were mainly caused by direct emissions. The higher HONO/NO_x ratios in urban areas also reflected higher contributions from direct emissions, while contributions of direct emissions were not significant in suburban areas. Moreover, the nocturnal HONO/NO_2 ratios, as a representa-

tive of the heterogeneous reaction efficiencies, were 0.038 and 0.103 on average in urban and suburban areas, respectively. The higher HONO/NO_2 indicated a higher NO_2 conversion efficiency in suburban areas. Moreover, the correlations of HONO/NO_2 vs. *RH* and HONO/NO_2 vs. $PM_{2.5}$ concentrations showed *RH* and particle concentrations could affect the NO_2 conversion. When *RH* was below 85%, the HONO/NO_2 ratios increased with the *RH* increasing, when *RH* was higher than 85%, the HONO/NO_2 would decline. Similarly, when $PM_{2.5}$ concentrations were below 100 $\mu g/m^3$, the HONO/NO_2 ratios increased with the $PM_{2.5}$ concentrations increasing. However, the decrease in HONO/NO_2 ratios when $PM_{2.5}$ concentrations were higher than 100 $\mu g/m^3$ was caused by the high *RH*, due to excess water limiting the conversion of NO_2 and dissolution of HONO. At last, the net productions of homogeneous reactions of nighttime were compared. Due to extremely high concentrations of NO, the contributions of homogeneous reactions productions would be significant in HONO formations in urban areas.

1   Lammel G, Cape JN. Nitrous acid and nitrite in the atmosphere. *Chem Soc Rev*, 1996, 25: 361–369

2   Harrison RM, Peak JD, Collins GM. Tropospheric cycle of nitrous acid. *J Geophys Res*, 1996, 101: 14429–14439

3   Kleffmann J, Kurtenbach R, Lorzer J, Wiesen P, Kalthoff N, Vogel B, Vogel H. Measured and simulated vertical profiles of nitrous acid. Part I: field measurements. *Atmos Environ*, 2003, 37: 2949–2955

4   Alicke B, Platt U, Stutz J. Impact of nitrous acid photolysis on the total hydroxyl radical budget during the limitation of oxidant production/pianura padana produzione di ozono study in Milan. *J Geophys Res*, 2002, 107: LOP 9-1–LOP 9-17

5   Kurtenbach R, Becker KH, Gomes JAG, Kleffmann J, Lorzer JC, Spittler M, Wiesen P, Ackermann R, Geyer A, Platt U. Investigations of emissions and heterogeneous formation of HONO in a road traffic tunnel. *Atmos Environ*, 2001, 35: 3385–3394

6   Kirchstetter TW, Harley RA, Littlejohn D. Measurement of nitrous acid in motor vehicle exhaust. *Environ Sci Technol*, 1996, 30: 2843–2849

7   Li X, Brauers T, Haseler R, Bohn B, Fuchs H, Hofzumahaus A. Exploring the atmospheric chemistry of nitrous acid (HONO) at a rural site in southern China. *Atmos Chem Phys*, 2012, 12: 1497–1513

8   Grassian VH. Heterogeneous uptake and reaction of nitrogen oxides and volatile organic compounds on the surface of atmospheric particles including oxides, carbonates, soot and mineral dust: Implications for the chemical balance of the troposphere. *Int Rev Phys Chem*, 2001, 20: 467–548

9   Ammann M, Kalberer M, Jost DT, Tobler L, Rössler E, Piguet D, Gäggeler HW, Baltensperger U. Heterogeneous production of nitrous acid on soot in polluted air masses. *Nature*, 1998, 395: 157–160

10   Finlayson-Pitts BJ, Wingen LM, Sumner AL, Syomin D, Ramazan KA. The heterogeneous hydrolysis of NO_2 in laboratory systems and in outdoor and indoor atmospheres: an integrated mechanism. *Phys Chem Chem Phys*, 2003, 5: 223–242

11   Stutz J, Alicke B, Ackermann R, Geyer A, Wang SH, White AB, Williams EJ, Spicer CW Jr, Fast JD. Relative humidity dependence

Table 3   Comparison of different pathways of HONO formation in urban and suburban areas during the nighttime [a]

	HONO (ppbv)	Direct emission (%)	Net homogeneous production (%)	The rest contributions (%)	Heterogeneous reaction (HONO/NO_2)
Urban	1.78	39.6	42.2	18.2	0.038
Suburban	0.70	8.5	10.6	80.9	0.103

a) All data were calculated by averaging the concentrations of Oct. 28–Oct. 31.

of HONO chemistry in urban areas. *J Geophys Res*, 2004, 109: D03307

12 Acker K, Febo A, Trick S, Perrino C, Bruno P, Wiesen P, Moller D, Wieprecht W, Auel R, Giusto M, Geyer A, Platt U, Allegrini I. Nitrous acid in the urban area of Rome. *Atmos Environ*, 2006, 40: 3123–3133

13 Calvert JG, Yarwood G, Dunker AM. An evaluation of the mechanism of nitrous-acid formation in the urban atmosphere. *Res Chem Intermediat*, 1994, 20: 463–502

14 Hao N, Zhou B, Chen D, Chen LM. Observations of nitrous acid and its relative humidity dependence in Shanghai. *J Environ Sci (China)*, 2006, 18: 910–915

15 Hendrick F, Muller JF, Clemer K, Wang P, De Mazière M, Fayt C, Gielen C, Hermans C, Ma JZ, Pinardi G, Stavrakou T, Vlemmix T, van Roozendael M. Four years of ground-based max-DOAS observations of HONO and NO$_2$ in the Beijing area. *Atmos Chem Phys*, 2014, 14: 765–781

16 Qin M, Xie P, Su H, Gu JW, Peng FM, Li SW, Zeng LM, Liu JG, Liu WQ, Zhang YH. An observational study of the HONO-NO$_2$ coupling at an urban site in Guangzhou city, south China. *Atmos Environ*, 2009, 43: 5731–5742

17 Qin M, Xie PH, Liu WQ, Li A, Dou K, Fang W, Liu JG, Zhnag WJ. Observation of atmospheric nitrous acid with DOAS in Beijing, China. *J Environ Sci-China*, 2006, 18: 69–75

18 Spataro F, Ianniello A, Esposito G, Allegrini I, Zhu T, Hu M. Occurrence of atmospheric nitrous acid in the urban area of Beijing (China). *Sci Total Environ*, 2013, 447: 210–224

19 Stutz J, Alicke B, Neftel A. Nitrous acid formation in the urban atmosphere: gradient measurements of NO$_2$ and HONO over grass in Milan, Italy. *J Geophys Res*, 2002, 107: LOP 5

20 Su H, Cheng YF, Cheng P, Zhang YH, Dong SF, Zeng LM, Wang XS, Slanina J, Shao M, Wiedensohler A. Observation of nighttime nitrous acid (HONO) formation at a non-urban site during pride-PRD2004 in China. *Atmos Environ*, 2008, 42: 6219–6232

21 Su H, Cheng YF, Shao M, Gao DF, Yu ZY, Zeng LM, Slanina J, Zhang YH, Wiedensohler A. Nitrous acid (HONO) and its daytime sources at a rural site during the 2004 pride-PRD experiment in China. *J Geophys Res*, 2008, doi: 10.1029/2007JD009060

22 Vogel B, Vogel H, Kleffmann J, Kurtenbach R. Measured and simulated vertical profiles of nitrous acid. Part II. Model simulations and indications for a photolytic source. *Atmos Environ*, 2003, 37: 2957–2966

23 Wang SS, Zhou R, Zhao H, Wang ZR, Chen LM, Zhou B. Long-term observation of atmospheric nitrous acid (HONO) and its implication to local NO$_2$ levels in Shanghai, China. *Atmos Environ*, 2013, 77: 718–724

24 Wong KW, OH HJ, Lefer BL, Rappengluck B, Stütz J. Vertical profiles of nitrous acid in the nocturnal urban atmosphere of Houston, TX. *Atmos Chem Phys*, 2011, 11: 3595–3609

25 Yu Y, Galle B, Panday A, Hodson E, Prinn R, Wang S. Observations of high rates of NO$_2$-HONO conversion in the nocturnal atmospheric boundary layer in Kathmandu, Nepal. *Atmos Chem Phys*, 2009, 9: 6401–6415

26 Wang YS, Yao L, Wang LL, Liu ZR, Ji DS, Tang GQ, Zhang JK, Sun Y, Hu B, Xin JY. Mechanism for the formation of the January 2013 heavy haze pollution episode over central and eastern China. *Sci China Earth Sci*, 2014, 57: 14–25

27 Sun YL, Jiang Q, Wang ZF, Fu PF, Li J, Yang T, Yin Y. Investigation of the sources and evolution processes of severe haze pollution in Beijing in January 2013. *J Geophys Res*, 2014, 119: 4380–4398

28 Quan J, Tie X, Zhang Q, Liu Q, Li X, Gao Y, Zhao D. Characteristics of heavy aerosol pollution during the 2012–2013 winter in Beijing, China. *Atmos Environ*, 2014: 83–89

29 Chen P, Zhang Q, Quan J, Gao Y, Huang MY. Temporal and spatial distribution of ozone concentration by aircraft sounding over Beijing (in Chinese). *Chinese J Environ Sci*, 2012: 4141–4150

30 Kleffmann J, Heland J, Kurtenbach R, Lorzer J, Wiesen P. A new instrument (LOPAP) for the detection of nitrous acid (HONO). *Environ Sci Pollut R*, 2002, 4: 48–54

31 Huang G, Zhou XL, Deng GH, Qiao HC, Civerolo K. Measurements of atmospheric nitrous acid and nitric acid. *Atmos Environ*, 2002, 36: 2225–2235

32 Heland J, Kleffmann J, Kurtenbach R, Wiesen P. A new instrument to measure gaseous nitrous acid (HONO) in the atmosphere. *Environ Sci Technol*, 2001, 35: 3207–3212

33 Wojtal P, Halla JD, McLaren R. Pseudo steady states of HONO measured in the nocturnal marine boundary layer: a conceptual model for HONO formation on aqueous surfaces. *Atmos Chem Phys*, 2011, 11: 3243–3261

34 Spataro F, Ianniello A. Sources of atmospheric nitrous acid: state of the science, current research needs, and future prospects. *J Air Waste Manage*, 2014, 64: 1232–1250

35 Lu KD, Rohrer F, Holland F, Fuchs H, Bohn B, Brauers T, Chang CC, Häseler R, Hu M, Kita K, Kondo Y, Li X, Lou SR, Nehr S, Shao M, Zeng LM, Wahner A, Zhang YH, Hofzumhaus A. Observation and modelling of OH and HO$_2$ concentrations in the pearl river delta 2006: a missing oh source in a VOC rich atmosphere. *Atmos Chem Phys*, 2012, 12: 1541–1569